



Paths to light trapping in thin film GaAs solar cells

JIANLING XIAO,¹ HANLIN FANG,¹ RONGBIN SU,¹ KEZHENG LI,² JINDONG SONG,³ THOMAS F. KRAUSS,² JUNTAO LI,^{1,*} AND EMILIANO R. MARTINS⁴

¹State Key Laboratory of Optoelectronic Materials and Technologies, School of Physics, Sun Yat-sen University, Guangzhou, 510275, China

²Department of Physics, University of York, York, YO10 5DD, UK

³Center for Opto-Electronic Materials and Devices Research Post-Si Semiconductor Institute, Korea Institute of Science and Technology, Seoul, 02-791, South Korea

⁴São Carlos School of Engineering, Department of Electrical and Computer Engineering, University of São Paulo, Av. Trabalhador São-carlense, 400, São Carlos-SP, Brazil

*lijt3@mail.sysu.edu.cn

Abstract: It is now well established that light trapping is an essential element of thin film solar cell design. Numerous light trapping geometries have already been applied to thin film cells, especially to silicon-based devices. Less attention has been paid to light trapping in GaAs thin film cells, mainly because light trapping is considered less attractive due to the material's direct bandgap and the fact that GaAs suffers from strong surface recombination, which particularly affects etched nanostructures. Here, we study light trapping structures that are implemented in a high-bandgap material on the back of the GaAs active layer, thereby not perturbing the integrity of the GaAs active layer. We study photonic crystal and quasi-random nanostructures both by simulation and by experiment and find that the photonic crystal structures are superior because they exhibit fewer but stronger resonances that are better matched to the narrow wavelength range where GaAs benefits from light trapping. In fact, we show that a 1500 nm thick cell with photonic crystals achieves the same short circuit current as an unpatterned 4000 nm thick cell. These findings are significant because they afford a sizeable reduction in active layer thickness, and therefore a reduction in expensive epitaxial growth time and cost, yet without compromising performance.

© 2018 Optical Society of America under the terms of the [OSA Open Access Publishing Agreement](#)

OCIS codes: (050.0050) Diffraction and gratings; (050.5298) Photonic crystals; (220.0220) Optical design and fabrication; (220.4241) Nanostructure fabrication; (350.6050) Solar energy.

References and links

1. A. V. Geelen, P. R. Hageman, G. J. Bauhuis, P. C. V. Rijsingen, P. Schmidt, and L. J. Giling, "Epitaxial lift-off GaAs solar cell from a reusable GaAs substrate," *Mater. Sci. Eng. B* **45**(1-3), 162–171 (1997).
2. S. Chandrasekharan, K. Gomez, A. Al-Hourani, S. Kandeepan, T. Rasheed, L. Goratti, L. Reynaud, D. Grace, I. Bucaille, T. Wirth, and S. Allsopp, "Designing and implementing future aerial communication networks," *IEEE Commun. Mag.* **54**(5), 26–34 (2016).
3. M. A. Green, K. Emery, Y. Hishikawa, W. Warta, E. D. Dunlop, D. H. Levi, and A. W. Y. Ho-Baillie, "Solar cell efficiency tables (version 49)," *Prog. Photovolt. Res. Appl.* **25**, 144–150 (2017).
4. ALTADEVICES, "28.8% Conversion efficiency for single-junction solar cells under 1 sun illumination", retrieved <http://www.altadevices.com>.
5. S. Moon, K. Kim, Y. Kim, J. Heo, and J. Lee, "Highly efficient single-junction GaAs thin-film solar cell on flexible substrate," *Sci. Rep.* **6**(1), 30107 (2016).
6. J. Adams, V. Elarde, A. Hains, and C. Stender, "Demonstration of multiple substrate reuses for inverted metamorphic solar cells," in *Photovoltaic Specialists Conference*, 2012), 1–6.
7. K. Lee, J. D. Zimmerman, X. Xiao, K. Sun, and S. R. Forrest, "Reuse of GaAs substrates for epitaxial lift-off by employing protection layers," *J. Appl. Phys.* **111**(3), 033527 (2012).
8. D. M. Geum, M. S. Park, J. Y. Lim, H. D. Yang, J. D. Song, C. Z. Kim, E. Yoon, S. Kim, and W. J. Choi, "Ultra-high-throughput Production of III-V/Si Wafer for Electronic and Photonic Applications," *Sci. Rep.* **6**(1), 20610 (2016).
9. S. M. Lee, A. Kwong, D. Jung, J. Faucher, R. Biswas, L. Shen, D. Kang, M. L. Lee, and J. Yoon, "High Performance Ultrathin GaAs Solar Cells Enabled with Heterogeneously Integrated Dielectric Periodic Nanostructures," *ACS Nano* **9**(10), 10356–10365 (2015).

10. N. Vandamme, H. L. Chen, A. Gaucher, B. Behaghel, A. Lemaître, A. Cattoni, C. Dupuis, N. Bardou, J. F. Guillemoles, and S. Collin, "Ultrathin GaAs Solar Cells With a Silver Back Mirror," *IEEE J. Photovoltaics* **5**(2), 565–570 (2015).
11. J. Yoon, S. Jo, I. S. Chun, I. Jung, H. S. Kim, M. Meitl, E. Menard, X. Li, J. J. Coleman, U. Paik, and J. A. Rogers, "GaAs photovoltaics and optoelectronics using releasable multilayer epitaxial assemblies," *Nature* **465**(7296), 329–333 (2010).
12. E. Yablonovitch, T. Gmitter, J. P. Harbison, and R. Bhat, "Extreme selectivity in the lift-off of epitaxial GaAs films," *Appl. Phys. Lett.* **51**(26), 2222–2224 (1987).
13. M. M. A. J. Voncken, J. J. Schermer, A. T. J. V. Niftrik, G. J. Bauhuis, P. Mulder, P. K. Larsen, T. P. J. Peters, B. D. Bruin, A. Klaassen, and J. J. Kelly, "Etching AlAs with HF for Epitaxial Lift-Off Applications," *J. Electrochem. Soc.* **151**(5), G347–G352 (2004).
14. K. Lee, J. D. Zimmerman, T. W. Hughes, and S. R. Forrest, "Non-Destructive Wafer Recycling for Low-Cost Thin-Film Flexible Optoelectronics," *Adv. Funct. Mater.* **24**(27), 4284–4291 (2014).
15. S. B. Shim, J. S. Chun, S. W. Kang, S. W. Cho, S. W. Cho, Y. D. Park, P. Mohanty, N. Kim, and J. Kim, "Micromechanical resonators fabricated from lattice-matched and etch-selective GaAs/InGaP/GaAs heterostructures," *Appl. Phys. Lett.* **91**(13), 133505 (2007).
16. G. J. Bauhuis, P. Mulder, E. J. Haverkamp, J. J. Schermer, E. Bongers, G. Oomen, W. Köstler, and G. Strobl, "Wafer reuse for repeated growth of III-V solar cells," *Prog. Photovolt. Res. Appl.* **18**(3), 155–159 (2010).
17. L. Zeng, Y. Yi, C. Hong, J. Liu, N. Feng, X. Duan, L. C. Kimerling, and B. A. Alamariu, "Efficiency enhancement in Si solar cells by textured photonic crystal back reflector," *Appl. Phys. Lett.* **89**(11), 111111 (2006).
18. F. Priolo, T. Gregorkiewicz, M. Galli, and T. F. Krauss, "Silicon nanostructures for photonics and photovoltaics," *Nat. Nanotechnol.* **9**(1), 19–32 (2014).
19. D. Liang, Y. Kang, Y. Huo, Y. Chen, Y. Cui, and J. S. Harris, "High-Efficiency Nanostructured Window GaAs Solar Cells," *Nano Lett.* **13**(10), 4850–4856 (2013).
20. D. S. Kim, S. H. Eo, and J. H. Jang, "Direct integration of subwavelength structure on a GaAs solar cell by using colloidal lithography and dry etching process," *J. Vac. Sci. Technol. B Microelectron. Nanometer Struct. Process. Meas. Phenom.* **31**, 1202 (2013).
21. S. Collin, N. Vandamme, J. Goffard, A. Cattoni, A. Lemaître, and J. F. Guillemoles, "Ultrathin GaAs solar cells with a nanostructured back mirror," in *Photovoltaic Specialist Conference*, 2015), pp. 1–3.
22. H. L. Chen, A. Cattoni, N. Vandamme, J. Goffard, A. Lemaître, A. Delamarre, B. Behaghel, K. Watanabe, M. Sugiyama, and J. F. Guillemoles, "200nm-Thick GaAs solar cells with a nanostructured silver mirror," in *Photovoltaic Specialists Conference* (2016)
23. S. Saravanan, T. Krishna Teja, R. S. Dubey, and S. Kalainathan, "Design and analysis of GaAs thin film solar cell using an efficient light trapping bottom structure," *Materials Today: Proceedings* **3**, 2463–2467 (2016).
24. A. Mellor, N. P. Hylton, S. A. Maier, and N. Ekins-Daukes, "Interstitial light-trapping design for multi-junction solar cells," *Sol. Energy Mater. Sol. Cells* **159**, 212–218 (2017).
25. V. Ganapati, O. D. Miller, and E. Yablonovitch, "Light Trapping Textures Designed by Electromagnetic Optimization for Subwavelength Thick Solar Cells," *IEEE J. Photovoltaics* **4**(1), 175–182 (2014).
26. E. Huggins, *Introduction to Fourier Optics* (McGraw-Hill, 1968), pp. 97–101.
27. M. S. Tobin, *Introduction to Fourier Optics*, Second Edition, Joseph W. Goodman, ed. (American Scientist, 1997), pp. 581–582.
28. E. R. Martins, J. Li, Y. Liu, V. Depauw, Z. Chen, J. Zhou, and T. F. Krauss, "Deterministic quasi-random nanostructures for photon control," *Nat. Commun.* **4**, 2665 (2013).
29. J. Li, K. Li, C. Schuster, R. Su, X. Wang, B.-H. V. Borges, T. F. Krauss, and E. R. Martins, "Spatial resolution effect of light coupling structures," *Sci. Rep.* **5**(1), 18500 (2016).
30. B. M. Kayes, H. Nie, R. Twist, and S. G. Spruytte, "27.6% Conversion efficiency, a new record for single-junction solar cells under 1 sun illumination," in *Photovoltaic Specialists Conference*, 2011), 000004–000008.
31. B. Galiana, I. Reystolle, M. Baudrit, I. Garcia, and C. Algora, "A comparative study of BSF layers for GaAs-based single-junction or multijunction concentrator solar cells," *Semicond. Sci. Technol.* **21**(10), 1387–1392 (2006).
32. C. Algora, E. Ortiz, I. Rey-Stolle, V. Diaz, R. Pena, V. M. Andreev, V. P. Khvostikov, and V. D. Rumyantsev, "A GaAs solar cell with an efficiency of 26.2% at 1000 suns and 25.0% at 2000 suns," *IEEE Trans. Electron Dev.* **48**(5), 840–844 (2001).
33. G. J. Bauhuis, P. Mulder, E. J. Haverkamp, J. C. C. M. Huijben, and J. J. Schermer, "26.1% thin-film GaAs solar cell using epitaxial lift-off," *Sol. Energy Mater. Sol. Cells* **93**(9), 1488–1491 (2009).
34. J. J. Schermer, G. J. Bauhuis, P. Mulder, E. J. Haverkamp, J. V. Deelen, A. T. J. V. Niftrik, and P. K. Larsen, "Photon confinement in high-efficiency, thin-film III–V solar cells obtained by epitaxial lift-off," *Thin Solid Films* **511–512**, 645–653 (2006).
35. S. B. Mallick, M. Agrawal, and P. Peumans, "Optimal light trapping in ultra-thin photonic crystal crystalline silicon solar cells," *Opt. Express* **18**(6), 5691–5706 (2010).
36. D. Zhou and R. Biswas, "Photonic crystal enhanced light-trapping in thin film solar cells," *J. Appl. Phys.* **103**(9), 093102 (2008).
37. E. Battal, T. A. Yogurt, L. E. Aygun, and A. K. Okyay, "Triangular metallic gratings for large absorption enhancement in thin film Si solar cells," *Opt. Express* **20**(9), 9458–9464 (2012).

1. Introduction

III-V solar cells, e.g. those made of Gallium Arsenide (GaAs), have a high energy to weight ratio [1] which makes them excellent candidates for airborne applications such as unmanned aerial vehicles and high altitude platforms [2]. Their efficiency is the highest of any type of single junction solar cell with 28.8% (measured under the global AM1.5 spectrum (1000 W/m²) at 25 degrees Celsius (IEC 60904-3:2008, ASTM G-173-03 global)) [3, 4]. The benefit of this high efficiency, however, is offset by the higher costs compared to silicon solar cells, which has held back terrestrial applications.

Many methods have been proposed for improving the cost-effectiveness of GaAs solar cells while maintaining their high conversion efficiency. Amongst the many methods, two are particularly effective and practicable, namely: a) to reuse the GaAs substrate [5–8], or b) to decrease the thickness of the GaAs active layer [9, 10].

Regarding a), epitaxial lift-off (ELO) is already being used to transfer micrometer-thick device layers to another substrate by etching a sacrificial layer between the device's active epitaxial layer and the GaAs substrate [4]. Examples of such sacrificial layers are Aluminum Gallium Arsenide (Al_xGa_{1-x}As) and Indium Gallium Phosphide (In_xGa_{1-x}P), which can be selectively etched by Hydrofluoric Acid (HF) [11–13] and Hydrochloric Acid (HCl) [14, 15], respectively.

Once the ELO cost saving procedure [5–7, 16] has been implemented, the next costly processing step is the epitaxial growth of the subsequent solar cell on the recovered substrate. Therefore, if the active layer could be made thinner without loss of overall efficiency, further cost reduction was possible. We believe that light trapping structures can achieve this goal. The issue with light trapping structures in GaAs, however, is the high surface recombination velocity of the material. If the GaAs is patterned directly, the resulting surface damage leads to a significant deterioration in efficiency, as is well known [17, 18]. One way to circumvent this problem is to pattern the light trapping structure on other high bandgap materials either on the front [19, 20] or on the back of the solar cell [21–23]. The implementation on the back-side presents some advantages including the ability to separately optimise light trapping and anti-reflection coating (ARC) [24, 25]. Besides, nanostructures on the back side are typically thinner than in the front side [26, 27] because the former operates in reflection and the latter in transmission; this difference is a consequence of the dependence of the diffraction efficiency on the total optical path difference between grooves and ridges: since in reflection light propagates twice through the ridges and grooves, a structure operating in reflection with half of the height of a structure operating in transmission will exhibit the same optical path difference and, consequently, comparable diffraction efficiencies. Furthermore, patterning the light trapping structure in high bandgap material, such as InGaP and AlGaAs, has a much lower impact on the surface recombination compared to patterning directly in the absorbing layer [19] and their parasitic absorption is lower because the blue end of the spectrum is already being absorbed by the active layer, so does not get absorbed by the light trapping layer. Overall, we therefore propose to implement the nanostructure in an InGaP layer placed at the rear of the GaAs active layer.

Light trapping schemes for thin film solar cells are typically based on the excitation of waveguide modes in the active layer. The resonant nature of the waveguide-mode excitation then poses the challenge of achieving broadband and strong absorption enhancement. This problem has been intensively investigated in c-Si thin film solar cells, where it has been recognised that quasi-random nanostructures [28] are the most promising structures to maximise solar absorption. Despite their promise, quasi-random nanostructures have not yet been applied to GaAs solar cells. Therefore, the identification of the optimum light trapping nanostructure for GaAs solar cells remains an open problem which we address in this paper.

Our strategy is to compare structures with different k-space (spatial Fourier space) characteristics. Conducting the study in k-space is advantageous because it allows for the identification of the desired functional properties of the structure without making reference to

its specific geometrical details [28]. We start out by quantifying the benefit of light trapping for different active layer thicknesses. We then proceed by exploring the differences between two very different types of light trapping nanostructures, namely the simply periodic and the more complex quasi-random structures [28, 29]. Finally, we design, characterise and compare - both experimentally and theoretically - the absorption enhancement of a ~135 nm thick GaAs active layer using photonic crystals (PhCs) and quasi-random nanostructures on the back side of a GaAs layer.

2. Effect of light trapping as a function of active layer thickness

We first address the light trapping problem by theoretically investigating the effect of back-side light trapping as a function of active layer thickness.

Figure 1(a) shows the architecture of a GaAs solar cell placed on a silicon substrate [8] as an exemplar. The GaAs based p-n junction forms the active layer, on the top of which a 60 nm thick Si_3N_4 is deposited. The 30 nm n-InGaP and 50 nm p-InGaP layers act as the window and back surface field (BSF), respectively; it is this layer which will form the light trapping nanostructure in the next step. The top metal electrode is formed by a Ni/Au/Ge/Ni/Au stack [8]. The structure is terminated on the bottom by a Pt/Au metal layer (also acting as a bonding material) and the silicon substrate provides mechanical stability.

We begin by identifying the minimum active layer thickness required to fully absorb the incoming light without the need for light trapping. Figure 1(b) shows the calculated integrated absorption of the solar cell as a function of the GaAs active layer thicknesses for different wavelength ranges (400 nm–600 nm, 600 nm–900 nm and 400 nm–900 nm). The integrated absorption is defined as the total amount absorbed solar photons divided by the total amount of incoming solar photons. For the calculation, we used the AM1.5G spectrum. The mathematical expression for the integrated absorption is shown as Eq. (1):

$$Abs = \frac{\int_{400}^{900} A(\lambda) I(\lambda) \frac{\lambda}{hc} d\lambda}{\int_{400}^{900} I(\lambda) \frac{\lambda}{hc} d\lambda} \quad (1)$$

where $A(\lambda)$ is the absorptance of the cell, $I(\lambda)$ is the AM1.5G solar spectral density, h is the Planck constant, c is speed of light in vacuum and λ is the wavelength. Notice that the term $I(\lambda)\lambda/(hc)$ corresponds to the solar photon density.

The minimum thickness then corresponds to the point where the integrated absorption saturates, which is approximately 4 μm , shown as the orange dashed line in Fig. 1(b). We note that typical high performance single junction GaAs solar cells utilise active layer thicknesses of this order [5, 30–34].

The integrated absorption falls noticeably as the thickness is reduced below 1 μm , shown as the green dashed line in Fig. 1(b). For example, at 250 nm, the integrated absorption is 20% lower than its saturation value at 4 μm . This significant decline indicates that absorption enhancement through light trapping is particularly important for active layers thinner than 1 μm . Furthermore, this requirement is even more stringent in the red and near infrared (IR) wavelength range as highlighted by Fig. 1(b), which shows that it is the long wavelength range which limits the performance of thin cells.

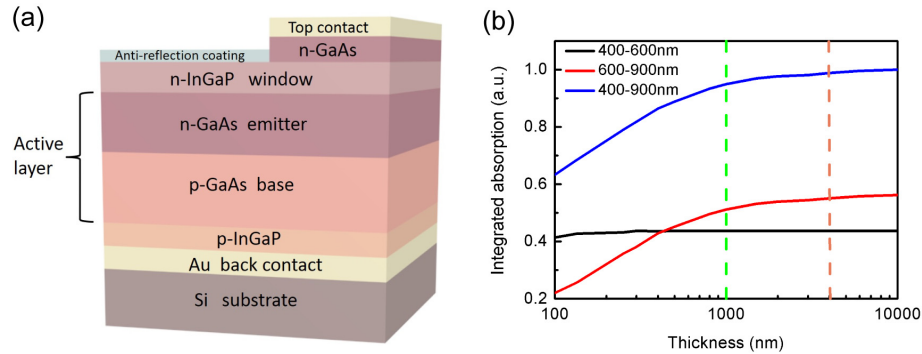


Fig. 1. (a) Structure of the GaAs solar cell and (b) its performance as a function of active layer thickness. The integrated absorption was calculated for different GaAs thicknesses in the wavelength regime of 400 nm-600 nm (black), 600 nm-900 nm (red) and 400 nm-900 nm (blue). A 60 nm layer of Si_3N_4 is applied as an ARC. The green dashed line highlights the thickness of 1 μm below which the absorption drops significantly. The orange dashed line highlights the thickness of 4 μm , above which the absorption no longer increases, which we refer to as the saturation thickness.

Having identified a saturation thickness of 4 μm , we proceed by investigating the effect of back-side light trapping as a function of active layer thickness. Figure 2(a) shows the structure with back-side patterning and Fig. 2(b) shows the integrated absorption with and without a light trapping structure (planar reflector). The light trapping structure is an optimised PhC which is patterned on the p-InGaP layer. The period, hole diameter and etch depth are 600 nm, 396 nm and 50 nm, respectively (details in the next section). Notice that the thickness of p-InGaP layer now is 60 nm and after patterned structure, there is a 10 nm thick InGaP to provide BSF. The holes of the PhC are filled with Au. As expected, the benefit of light trapping is stronger for thinner films. For example, for a 500 nm thin material, light trapping can boost 10.1% of the integrated absorption, whereas for 2000 nm, the difference is only 2.9%. Notice that the integrated absorption with light trapping for a thickness of 500 nm is almost the same as the integrated absorption without light trapping (planar reflector) for a thickness of 2000 nm. This means that, for achieving the same integrated absorption of a 2000 nm cell, light trapping allows a reduction of 1500 nm in the active GaAs layer thickness. For the typical high performance single junction GaAs solar cells [5, 30–32], light trapping allows a reduction of 2500 nm (from 4000 nm without light trapping (planar reflector) to 1500 nm with light trapping). These results clearly indicate that a significant amount of material can be saved, and therefore that the cost of epitaxial growth can be substantially reduced by applying light trapping to the back-side of the solar cell, and, most importantly, without a drop in absorption.

Next, we select a single active-layer thickness to compare the performance of PhCs and quasi-random structures. We choose a relatively low material thickness of 135 nm for the comparison to amplify the differences between the two types of nanostructure.

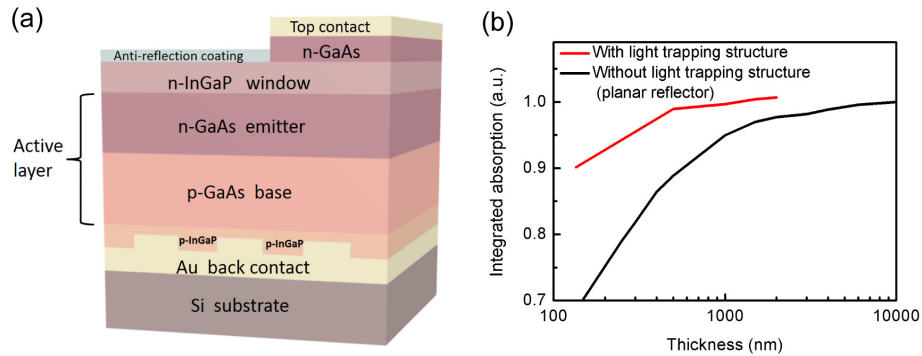


Fig. 2. (a) Structure of the GaAs solar cell on silicon substrate with light trapping nanostructure. (b) Calculated integrated absorption of a GaAs solar cell with (red) and without (black) light trapping structure (planar reflector) applied, as a function of GaAs thickness.

3. Photonic crystal vs quasi-random light trapping nanostructure

As we have previously demonstrated, the quasi-random approach offers the highest light trapping efficiency of any nanostructure when applied to a thin film silicon solar cell [28], which exploits the fact that there are only very few propagating modes in the active layer [29]. We note that the quasi-random approach is particularly well suited to broadband light trapping, which is essential for silicon due to its indirect bandgap. The question is now whether the result for GaAs is similar or whether the direct bandgap of GaAs has an impact on the optimum type of nanostructure.

In order to quantify the absorption enhancement in a wide wavelength range (600-900 nm) of the two types of nanostructure in light of the direct/indirect bandgap difference, we consider their k -space properties. We choose 725 nm as the operating wavelength, which sits in the centre of this range in terms of k -space. We calculate the dispersion curve of the corresponding mode and find that the k -value at 725 nm is $k = 10.5 \mu\text{m}^{-1}$. The period of structure can be obtained as $\Lambda = (2\pi)/k = 600$ nm, and this was our choice of period for the PhC structure.

While PhCs only have a few, but very strong k -space components [35, 36], the quasi-random structures offer a much richer k -space, which is the reason for their broadband light trapping properties. As for the quasi-random structure, we chose a period of 1600 nm. With this choice of period, the diffraction orders that can be excited in the wavelength range of interest are between 2nd~6th. We tested a range of diffraction orders and found that the optimum result was achieved for the 2nd~4th order, which corresponds to the range between 7.85 to $15.7 \mu\text{m}^{-1}$. According to the dispersion model, the range $7.85 - 15.7 \mu\text{m}^{-1}$ corresponds to wavelength in the range 675 – 750 nm.

The PhCs were optimised by changing the etch depth and diameter. The corresponding real space structure is shown in Fig. 3(a) and its k -space distribution is shown in Fig. 3(b).

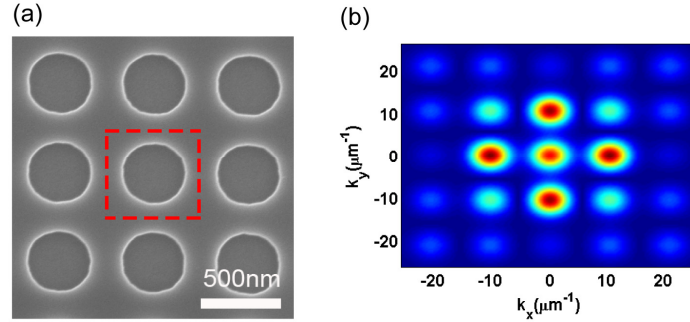


Fig. 3. (a) SEM of an optimised GaAs PhCs structure fabricated by electron beam lithography (EBL) and inductively coupled plasma (ICP) etching. One unit cell of the PhC structure is highlighted by the red square. The period, hole diameter and etch depth are 600 nm, 396 nm and 50 nm, respectively (b) Corresponding k-space distribution. The z component is the amplitude of the 2D Fourier transform of the structure.

The quasi-random structure was optimised in a similar way as described in [28], whereby the diffraction orders that can excite guided modes are enhanced while those that do not are suppressed. In order to ease the fabrication constraint, we chose a quasi-random structure whose unit cell contains 16x16 pixels. The 2nd~4th diffraction orders are maximised via a binary search optimization algorithm [28] and we concentrate the k-space energy in the range between 7.85 and 15.7 μm^{-1} , which is close to that of the PhC for ease of comparison (Fig. 3(b)). Finally, we optimise the etch depth to maximise the short-circuit current (J_{sc}) of the structure. The simulation employs a commercial FDTD code (Lumerical Inc, FDTD solutions) with periodic boundary conditions in x, y and perfectly matched layers (PML) in z. Notice that the structure exhibits an amorphous-like k-space energy distribution which resembles a ring (Fig. 4(b)). It also has more Fourier components than the PhC, thus offering a more broad-band light trapping effect; furthermore, the k-space components lie in the spectral region that enable waveguide-mode coupling as desired [29]. The real space distribution of the resulting quasi-random structure is shown in Fig. 4(a), with its k-space distribution shown in Fig. 4(b).

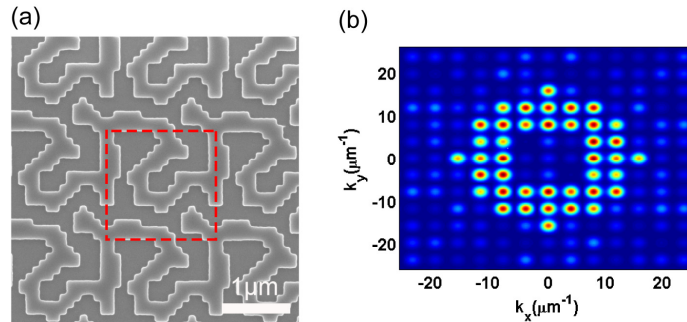


Fig. 4. (a) SEM micrograph of the optimised GaAs quasi-random structure fabricated by EBL and ICP etching. One unit cell with 16x16 pixels of the quasi-random structure is highlighted by the red square. The period and etch depth are 1600 nm and 50 nm. (b) Corresponding Fourier distribution. The z component is the amplitude of the 2D Fourier transform of the structure.

First, we compare the structures numerically. Figure 5 shows the absorption of a 135 nm thick GaAs layer with and without light trapping structures (planar reflector), including 4000 nm thick cells for reference, as well as the 1500 nm thick cell with photonic crystal to highlight its comparable performance. Table 1 shows the calculated J_{sc} as a function of the

GaAs layer thicknesses. The corresponding J_{sc} values are calculated by integrating the solar AM1.5G spectrum as shown in Eq. (2), where e is electronic charge, λ is incident wavelength, h is Planck's constant, c is speed of light, $I(\lambda)$ is the AM1.5G solar spectral density and $A(\lambda)$ is the absorption coefficient obtained from measurement or simulation as $A(\lambda) = 1 - R(\lambda)$.

$$J_{sc} = \frac{e}{hc} \int_{400}^{900} I(\lambda) A(\lambda) \lambda d\lambda \quad (2)$$

Table 1. Calculated J_{sc} values for GaAs solar cells of different GaAs thickness with and without light trapping structures.

	With PhC nanostructure		With Quasi-random nanostructure		Without light trapping structure (planar reflector)	
Thickness of GaAs layer (nm)	135	1500	135	1500	135	4000
J_{sc} of GaAs (mA/cm ²)	17.0	25.9	16.7	25.7	13.5	26.1

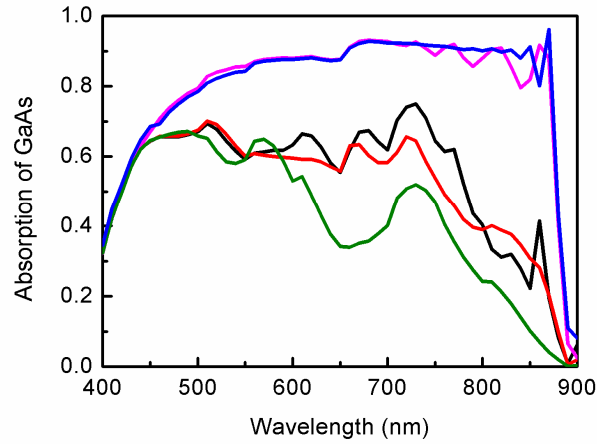


Fig. 5. The lower set of three curves compares the absorption of without light trapping structure (planar reflector) (green), quasi-random (red) and photonic crystal (black) 135 nm thick GaAs, highlighting the superiority of the photonic crystal pattern even at very low thickness. The upper set of two curves compares 4000 nm thick without light trapping structure (planar reflector) GaAs (blue) with photonic crystal patterned 1500 nm thick GaAs (magenta) to demonstrate their comparable performance.

The richer k-space energy distribution of quasi-random structures is most beneficial for thin absorbing layers, as these will have only a few guided modes. Thicker films, in contrast, support many guided modes, thus not requiring a rich k-space distribution to be accessed. Therefore, the comparison between PhC and quasi-random can be most conveniently performed using a very thin absorbing layer: if the PhC outperforms the quasi-random for a very thin absorbing layer, then the PhC is best (or at least equal) for all thicknesses. If, on the contrary, the quasi-random outperforms the PhC for very thin layers, then it remains to be identified how thick the absorbing layer should be so that the two systems perform comparably.

As shown in Fig. 5 and Table 1, the light trapping effect of a PhC in a very thin (135 nm thick) GaAs layer is already stronger than that of a quasi-random structure; the PhC achieves 17.0 mA/cm² while the quasi-random achieves 16.7 mA/cm². So we can confidently conclude that the PhC is the better structure for light trapping in GaAs solar cells. Furthermore, as shown in Table 1, the difference in J_{sc} reduces for thicker films, but the PhC still outperforms the quasi-random. Notice that there is a pronounced peak between 700 and 750 nm (black

curve of Fig. 5), resulting from the excitation of the guided mode and illustrating our choice of operating wavelength.

Therefore, contrary to what we have observed in crystalline silicon, GaAs cells benefit more from a simple periodic structure than from a structure with broadband light trapping properties such as the quasi-random. The reason for this counter-intuitive behavior is the direct bandgap and correspondingly narrowband wavelength range of weak absorption where GaAs benefits from light trapping. For a direct bandgap material, a narrowband, but strongly peaked absorption enhancement as provided by the PhC is hence called for. We note that a similar conclusion has been reached via an electromagnetic optimisation algorithm [25]; we now provide a different physical explanation for this observation.

In order to verify these observations experimentally, we have realised the light trapping designs of Figs. 3 and 4 on the rear of a 135 nm thick GaAs absorber layer. We added a 55 nm thick Si_3N_4 layer on the front for ARC and a 400 nm thick Au layer at the back for back reflection.

Figure 6 shows the fabrication steps. The sample consists of a 135 nm thick GaAs layer, an $\text{Al}_{0.7}\text{Ga}_{0.3}\text{As}$ sacrificial layer and GaAs substrate, all grown by molecular beam epitaxy (MBE). The PhC and quasi-random light trapping structures are patterned by EBL then etched by ICP for 50 nm; subsequently, a 400 nm thick Au layer is deposited on the surface of the GaAs film by electron beam evaporation and ion beam sputtering, followed by annealing at 200 degrees for 2 hours. The completed cell is then transferred to a glass substrate using Norland Optical Adhesive 61. Finally, the wafer is thinned and the $\text{Al}_{0.7}\text{Ga}_{0.3}\text{As}$ sacrificial layer is removed by a 10% solution of HF before a 55 nm thick Si_3N_4 layer is deposited by Inductively Coupled Plasma Chemical Vapor Deposition (ICPCVD) on the top for ARC.

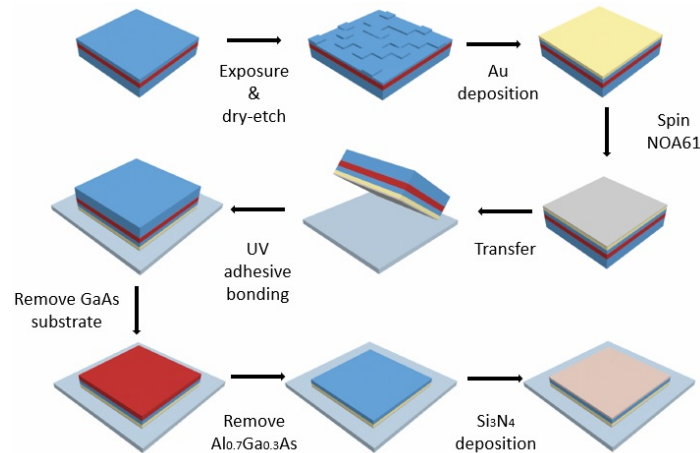


Fig. 6. The fabrication process steps required to fabricate the light trapping nanostructure on the rear of a 135 nm thick GaAs absorber layer.

To assess the performance experimentally, we measured the reflectivity with a white light laser source, an integrating sphere and a spectrograph. The absorption A is readily obtained from the reflectivity R as $A = 1 - R$. Figures 7(a) and 7(b) show the calculated and measured absorption with the PhC and quasi-random nanostructure applied, respectively. The FDTD simulation (Lumerical Inc, FDTD solutions) allows us to separate the beneficial absorption in GaAs from the parasitic absorption in the metal by using a mesh of 2 nm grid size and adding an analysis group into the 135 nm thick GaAs layer [37]. We note similar trends between the calculation and the experiment by including the parasitic absorption of the Au layer. Note that these curves are different from the corresponding curves in Fig. 5, because the experimental structure does not include the InGaP layer, which exhibits strong absorption between 400 nm

and 500 nm. As we are focusing on the optical properties, we did not use the InGaP layer in the experiment because its refractive index is very close to that of GaAs.

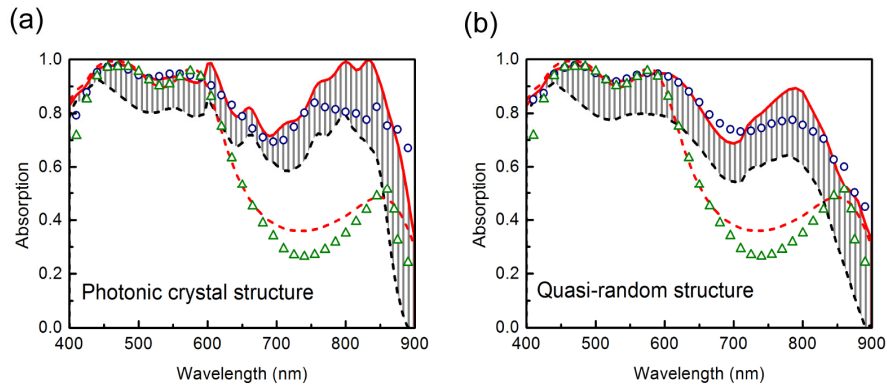


Fig. 7. Comparison between measured (blue circles) and calculated (red solid line) absorption of the experimental structure (a) with PhC structure and (b) with quasi-random structure. The calculated absorption of the GaAs layer corresponding to each structure is shown by black dashed line. The area between the black dashed and red solid lines correspond to parasitic absorption in the Au layer, which the experiment cannot separate. The measured and calculated absorption of a 135 nm thick GaAs layer without light trapping (planar reflector) is also shown for reference by the green triangle symbols and the red dashed line.

Figure 7(a) (with PhC) and 7(b) (with quasi-random) confirm that light trapping via excitation of guided modes is very effective to boost the absorption between 600 nm and 900 nm wavelength. Furthermore, the measured PhC absorption is higher than the quasi-random. For example, the measured absorption at 850 nm is ~80% for the PhC and ~60% for the quasi-random. Therefore, the experimental results confirm the conclusion already reached numerically, namely that the PhC is the best class of structure for light trapping in GaAs solar cells.

4. Conclusion

We have investigated and quantified the benefit of back-side light trapping in GaAs solar cells, comparing the light trapping effect between a photonic crystal and a quasi-random structure. Surprisingly, and in contrast to the case of silicon, the PhC structure outperforms the quasi-random nanostructure. We associate this difference to the difference in electronic band structure, namely the direct bandgap of the GaAs solar cell, which has a much narrower wavelength region where the absorption is weak and light trapping can be beneficially employed. PhCs, which feature few but strong resonance peaks, can be designed to exhibit resonant absorption in this specific wavelength region and thereby maximise the light trapping effect. In contrast, the broadband light trapping property of quasi-random nanostructures offers little benefit in this scenario, and in contrast, it dilutes the light trapping benefit. Hence, simply periodic structures such as PhCs due to their narrow but strong absorption resonances outperform multiperiodic structures such as the quasi-random. As a result, we show that a 1500 nm thick cell patterned with a photonic crystal can achieve the same short circuit current as a 4000 nm thick unpatterned cell, which affords a significant saving in terms of layer thickness and therefore in terms of epitaxial growth time. These conclusions are supported by simulations and experiments and are important for directing research into light trapping and cost reduction of thin-film GaAs solar cells.

Funding

National Natural Science Foundation of China (NSFC) (11674402, 11761131001); Ministry of Science and Technology of China (2016YFA0301300); Guangzhou science and

technology projects (201607010044, 201607020023), Natural Science Foundation of Guangdong (2016A030312012); Three Big Constructions—Supercomputing Application Cultivation Project (Sponsored by National Supercomputer Center In Guangzhou), the Fundamental Research Funds for the Central Universities, and EPSRC of U.K. under Grant EP/J01771X/1 (Structured Light). JDS acknowledges the support from the institutional program of KIST including flag-ship.

Acknowledgments

We acknowledge Lin Liu, Lidan Zhou, Chunchuan Yang, Zhenpeng Zhou, Beimeng Yao and Hongji Li for valuable discussions of experiment.